MSC-07230
Supplement 3

# APOLLO 16 MISSION REPORT

## SUPPLEMENT 3

## ASCENT PROPULSION SYSTEM FINAL FLIGHT EVALUATION

PREPARED BY

TRW Systems

APPROVED BY

Glynn S. Lunney
Manager, Apollo Spacecraft Program

(NASA-CR-134366) APOLLO 16, LM-11 ASCENT PROPULSION SYSTEM FINAL FLIGHT EVALUATION (TRW Systems) 55 p HC $5.75 CSCL 22C

N74-32254

Unclas
G3/30 44759

NATIONAL AERONAUTICS AND SPACE ADMINISTRATION

LYNDON B. JOHNSON SPACE CENTER

HOUSTON, TEXAS

June 1974

PROJECT TECHNICAL REPORT

# APOLLO 16

## LM-11
## ASCENT PROPULSION SYSTEM
## FINAL FLIGHT EVALUATION

NAS 9-12330

February 1973

Prepared for
NATIONAL AERONAUTICS AND SPACE ADMINISTRATION
MANNED SPACECRAFT CENTER
HOUSTON, TEXAS

Prepared by
W. G. Griffin
Systems Evaluation Department

NASA

Concurred by: _____
Z. D. Kirkland, Head
Systems Analysis Section

Concurred by: _____
E. C. Currie, Manager
Ascent Propulsion
Subsystem

Concurred by: _____
C. W. Yodzis, Chief
Primary Propulsion
Branch

TRW SYSTEMS

Approved by: _____
R.K.M. Seto, Manager
Task E-99B

Approved by: _____
J. M. Richardson, Head
Applied Mechanics
Section

Approved by: _____
R. K. Petersburg,
Manager, Systems
Evaluation Department

CONTENTS



TABLES

CONTENTS (Continued)

Page

ILLUSTRATIONS

CONTENTS (Continued)

# 1. PURPOSE AND SCOPE

The purpose of this report is to present the results of the postflight analysis of the Ascent Propulsion System (APS) performance during the Apollo 16 Mission. It is a supplement to the Apollo 16 Mission Report. Determination of the APS steady-state performance under actual flight environmental conditions was the primary objective of the analysis. Included in the report is such information as required to provide a comprehensive description of APS performance during the Apollo 16 Mission.

Major additions and changes to the preliminary results presented in the mission report (Reference 1) are listed below.

1) Calculated performance values for the APS lunar liftoff burn
2) Discussion of analysis techniques, problems and assumptions
3) Comparison of postflight analysis and preflight prediction
4) Reaction Control System (RCS) duty cycle included in the APS performance analysis
5) Transient performance analysis
6) The APS propellant consumption values have been revised as shown in Table 2

## 2. SUMMARY

The duty cycle for the LM-11 APS consisted of two firings, an ascent stage liftoff from the lunar surface and the Terminal Phase Initiation (TPI) burn. APS performance for the first firing was evaluated and found to be satisfactory. No propulsion data were received from the second APS burn; however, all indications were that the burn was nominal.

Engine ignition for the APS lunar liftoff burn occurred at the Apollo elapsed time (AET) of 175:31:47.9 (hours:minutes:seconds). Burn duration was 427.7 seconds.

Average steady-state engine performance parameters for the burn are as follows:

Thrust -3544 lbf

Isp - 311.8 sec

Mixture Ratio - 1.594

All performance parameters were well within their 3-sigma limits. Calculated throat erosion at engine cutoff for the ascent burn was approximately 2 percent greater than predicted.

## 3. INTRODUCTION

The APS duty cycle for the Apollo 16 Mission consisted of a lunar liftoff burn and a Terminal Phase Initiation (TPI) burn. Total burn duration for the two firings was 430.2 seconds. The Apollo 16/LM-11/APS was equipped with Rocketdyne Engine S/N 0013C. APS engine performance characterization equations used in preflight analyses and as a basis for the postflight evaluation are found in Reference 2. Engine acceptance test data used in the determination of performance are from Reference 3. Physical characteristics of the engine and feed system are presented in Table 1.

The APS lunar liftoff burn was preceded by five Service Propulsion System (SPS) burns and a Descent Propulsion System (DPS) firing. Ignition time for the initial APS firing was 175:31:47.9 AET. Engine cutoff was commanded at 175:38:55.6 AET for an APS burn duration of 427.7 seconds. Loss of signal (LOS) occurred following engine shutdown for the lunar liftoff burn at approximately 176:11 AET as the vehicle went behind the moon. The second APS burn was the 2.5 second Terminal Phase Initiation (TPI) maneuver. APS engine ignition time for the TPI maneuver was 176:26:05 AET, approximately 15 minutes after LOS. A summary of data concerning ascent stage main engine ignition and cutoff times and the associated velocity changes are shown below:

| Burn | Ignition AET (hr:min:sec) | Engine Cutoff AET (hr:min:sec) | Burn Duration (seconds) | Velocity (1) Change (ft/sec) |
|---|---|---|---|---|
| Lunar Liftoff | 175:31:47.9 | 175:38:55.6 | 427.7 | 6054.2 |
| TPI | 176:26:05 | 172:26:07.5 | 2.5 | 78.0 |

(1) Reference 1

## 4. STEADY-STATE PERFORMANCE ANALYSIS

### Analysis Technique

Determination of APS steady-state performance during the lunar orbit insertion burn was the primary objective of the LM-11 postflight analysis. The insertion burn duration was 427.7 seconds, engine on to engine off command.

The APS postflight analysis was conducted using the Apollo Propulsion Analysis Program (PAP) as the primary computational tool. Additionally, the Ascent Propulsion Subsystem Mixture Ratio Program (MRAPS) was used in an iterative technique with PAP to assist in the determination of the vehicle propellant mixture ratio. Reference 4 presents a detailed explanation of the operation of the MRAPS program and the underlying theory which it implements.

An initial estimate of the ascent stage weight at lunar liftoff of 10949 lbm was obtained from Reference 5. Ascent stage damp weight (total spacecraft weight less APS propellants) was considered to be constant throughout the burn, except for a 0.03 lbm/sec overboard flow rate which accounts for ablative nozzle erosion.

LM/RCS propellant usage and thrust histories were obtained from an analysis of the RCS bi-level measurements. Approximately 97 percent of the RCS consumption during the ascent burn was from the APS tanks. The remaining RCS usage, $\sim$2 lbm, was from the RCS tanks following the closing of the APS/RCS interconnect valves. Table 2 presents a summary of propellant usage,

including RCS consumption, from the APS tanks during the ascent burn. Propellant densities used in the program were based on equations from Reference 6, adjusted by measured density data for the LM-11 flight given in the Spacecraft Operational Data Book (SODB), Reference 7. Oxidizer and fuel temperatures were taken from flight measurement data and were 68.75°F and 70.75°F, respectively. These temperatures were considered to be constant throughout the segment of burn analyzed. The following flight measurement data were used in the analysis of the LM-11 APS burn: engine chamber pressure, engine interface pressures, vehicle thrust acceleration, propellant tank bulk temperatures, helium regulator outlet pressures, engine on-off commands, helium tank pressure measurements, and RCS thruster solenoid bi-level measurements. Measurement numbers and data pertinent to the above measurements, with the exception of RCS bi-levels, are given in Table 3. Plots of measurement data versus time are presented in the appendix to this report.

## Flight Data Analysis and Results

A 385 second segment of the APS lunar liftoff burn was selected to be analyzed for the purpose of determining steady-state performance. The segment of the burn analyzed began at 175:31:58.0 AET, 10.1 seconds after ignition, and ended at 175:38:23.0 AET, 32.6 seconds prior to cutoff. The periods immediately following ignition and immediately prior to engine cutoff are not included in order to minimize any errors resulting from data filtering spans which included the start and shutdown transients. APS engine propellant consumption during the burn is presented in Table 2. Propellant consumption from engine on command to the start of the steady-state analysis segment and from the end of the steady-state analysis to

the beginning of chamber pressure decay was extrapolated from steady-state analysis results.

The primary engine performance determinations made during the LM-11 postflight analysis are as follows (all average values are over the 385 second period of steady-state analysis):

1) Average APS specific impulse was 311.8 seconds
2) Average APS mixture ratio was determined to be 1.594
3) Average APS thrust was 3544. lbf
4) Engine throat erosion was 2 percent greater than predicted at 395 seconds after ignition.

An extrapolation of the APS steady-state analysis to include the entire burn, with the exception of ignition and shutdown transients, resulted in an average specific impulse, thrust, and mixture ratio of approximately the same values as the 385 second burn segment. LM-11 APS performance was greater than predicted with the average engine specific impulse exceeding the predicted average value by 2.4 seconds.

The general solution approach used in the LM-11 flight evaluation was to calculate the vehicle weight (including propellant loads) for the beginning of the burn segment used to analyze steady-state performance and then allow the PAP to vary this weight and other selected performance parameters (state variables) in order to achieve an acceptable data match. The PAP simulations were made using the previously discussed APS engine characterization model driven by engine interface pressures. Raw flight interface pressure measurement data were first filtered with a sliding arc filter and then, because of excessive distortion, these data were further smoothed using a fifth degree curve fit.

Simulation of RCS activity was accomplished with a model that was developed from individual thruster "on" time. This technique has been used on previous APS reconstructions and is fully discussed in Reference 8.

Initial PAP simulation results based on the input data outlined in the beginning of this section indicated the predicted throat erosion was less than that required to match flight data. A revised throat erosion curve was calculated using the partial derivatives of throat area with respect to acceleration. This technique has been used during previous APS post-flight reconstructions and has yielded good results. The inclusion of this calculated throat area curve in the analysis program resulted in an excellent acceleration match with a near zero mean and no significant slope. The derived throat erosion was 2 percent greater than predicted at approximately 395 seconds after ignition. Figure 1 shows the calculated throat area curve in comparison with the predicted curve for LM-11.

An APS chamber pressure error model (Reference 9) derived from previous flight data was used in the analysis. In addition to this model an adjustment to the flight chamber pressure data was necessitated by the chamber pressure excursion discussed in Section 8. The chamber pressure match resulting from the PAP analysis is not as good as might have been expected. However, considering the additional uncertainty in the chamber pressure measurement resulting from the chamber pressure excursion, the match is considered to be acceptable. A 1.2 psi chamber pressure measurement bias was determined from the final PAP solution. The residual match shown in Figure 3 incorporates the error model, flight data adjustment and the bias.

Interface pressure measurement biases of approximately 0.8 psia and -0.5[1] psia for oxidizer and fuel, respectively, were determined from the PAP results. These biases are well within the measurement accuracy for both the oxidizer (GP 1503) and fuel (GP 1501) interface pressure measurements.

A vehicle weight reduction of 20 lbm was determined from the PAP reconstruction. The best estimate of total ascent stage weight at lunar liftoff is 10929 lbm.

The principal indicator of the accuracy of the postflight reconstruction is the matching of calculated and measured acceleration data. A measure of the quality of the match is given by the residual slope and intercept data as shown in Figure 2. These data represent the ordinate intercept and the slope of a linear fit to the residual data. The closer both of these numbers are to zero, the more accurate the match. The acceleration match achieved with the LM-11 postflight reconstruction was very good. The LM-11 flight reconstruction was, by all indications, an accurate simulation of actual flight performance.

Figures 2 through 9 show the principal performance parameters associated with the LM-11 postflight analysis. Four flight measurements were used as time varying input to the Propulsion Analysis Program. Two of these measurements, fuel and oxidizer interface pressures, were used as program drivers. The other two, acceleration and chamber pressure, were compared to calculated values by the program's minimum variance technique. The acceleration and

[1]As a convention in this report, a negative bias indicates that measured data was reading less than its true value.

chamber pressure measurements along with their residuals (measured data minus calculated) are presented in Figures 2 and 3, respectively. Figures 4 and 5 contain oxidizer and fuel interface pressure measurement data (after smoothing of the raw data), the curve fits of these data input to the Apollo Propulsion Analysis Program, and the residuals between the flight data and the curve fit interface pressures. Calculated steady-state values for thrust, specific impulse, and oxidizer and fuel flow rates are shown in Figures 6 through 9.

## Comparison with Preflight Performance Prediction

Predicted performance of the LM-11 APS is presented in Reference 10. The intention of the preflight performance prediction was to simulate APS performance under flight environmental conditions for the Mission J-2 duty cycle. No attempt was made in the preflight prediction to simulate RCS operation.

Table 4 presents a summary of actual and predicted APS performance during the ascent burn. Engine specific impulse determined by the post-flight reconstruction is greater than had been predicted but is still within the 3-sigma limits of $\pm$ 3.5 seconds presented in Reference 10. Comparisons of predicted and reconstructed values for specific impulse, thrust, and mixture ratio are presented in Figure 10 along with related 3-sigma dispersions. The variations in flight specific impulse, thrust and mixture ratio were within their respective 3-sigma dispersions.

## Engine Performance at Standard Interface Conditions

Expected APS engine flight performance was based on an engine characterization which utilized data obtained during engine and injector acceptance

tests. In order to allow actual engine performance variations to be separated from variations induced by feed system, pressurization system, and propellant temperature variations, the acceptance test data are adjusted to a set of standard interface conditions; thereby providing a common basis for comparison. Standard interface conditions are as follows:

| | |
|---|---|
| Oxidizer interface pressure, psia | 170. |
| Fuel interface pressure, psia | 170. |
| Oxidizer interface temperature, °F | 70. |
| Fuel interface temperature, °F | 70. |
| Oxidizer density, $lbm/ft^3$ | 90.21 |
| Fuel density, $lbm/ft^3$ | 56.39 |
| Thrust acceleration, lbf/lbm | 1. |
| Throat area, $in^2$ | 16.44 |

Analysis results (at 13 seconds from ignition) for the ascent burn corrected to standard interface conditions and compared to acceptance test values are shown below:

| | Acceptance Test Data | Flight Analysis Result | Percent Difference | 3-Sigma, Percent |
|---|---|---|---|---|
| Thrust, lbf | 3510.7 | 3537.4 | 0.8 | 3.0 |
| Specific Impulse, $\frac{lbf\text{-}sec}{lbm}$ | 309.6 | 312.0 | 0.8 | 1.1 |
| Mixture Ratio | 1.604 | 1.604 | 0.0 | 1.7 |

Reduction of engine performance to standard interface conditions and comparison with acceptance test values shows good agreement.

# 5. PRESSURIZATION SYSTEM

## Helium Utilization

The helium storage tanks were loaded with a nominal 13.2 lbm. There was no indication of leakage from the helium bottles during the mission and calculated usage, 8.4 lbm, was as expected.

## Helium Regulator Performance

Helium regulator performance was approximately as predicted. The Class I primary regulator controlled helium flow throughout the burn. No significant oscillations in regulator outlet pressure were noted.

## 6. PROPELLANT LOADING AND USAGE

APS propellant loads at earth lift-off for the LM-11 Mission were 3224.7 lbm of oxidizer and 2017.8 lbm of fuel. During the translunar coast phase of the mission a mechanical problem in one of the RCS helium regulators necessitated the transfer of approximately 44 lbm of oxidizer and 16 lbm of fuel from the RCS tanks to the APS tanks through the APS/RCS interconnect. The total APS propellant loads at lunar landing were 3268.7 lbm and 2033.8 lbm for oxidizer and fuel, respectively. Of these amounts 36.0 lbm of oxidizer and 15.9 lbm of fuel are considered to be unusable or consumed during transient engine operation. Nominally deliverable propellants at APS lift-off were 3232.7 lbm, oxidizer, and 2017.9 lbm, fuel. Propellant density samples taken at the time of loading showed an oxidizer density of 1.4818 gm/cc @ 4°C and a fuel density of 0.8979 gm/cc @ 25°C. Both densities were at a pressure of one atmosphere.

APS consumption during the lunar lift-off burn was 3042 lbm, oxidizer and 1901 lbm, fuel. Total RCS consumption, from the APS tanks through the APS/RCS interconnect, during the same period burn was 77 lbm. Except for approximately the last 10 seconds of the burn, all RCS consumption was through the APS/RCS interconnect. The TPI maneuver usage was estimated as 19 lbm of oxidizer and 11 lbm of fuel. A total of 208 lbm of oxidizer and 121 lbm of fuel remained on board at the second APS burn cutoff.

## 7. ENGINE TRANSIENT ANALYSIS

An analysis of the start and shutdown transients was performed with the primary intention of determining transient total impulse. Figures 11 and 12 are traces of engine chamber pressure, measurement GP2010, during start and shutdown of the lunar lift-off burn, respectively. No data were available from the TPI burn.

The time from ignition signal to 90 percent steady-state thrust was 0.334 seconds, well within the specification limit for unprimed starts of 0.450 seconds. Total start transient impulse was 27 lbf-sec. The chamber pressure overshoot exceeded the upper limit of the measurement range (150 psia); however, there were no indications of rough combustion or other abnormal performance.

Total impulse from engine cutoff signal to 10 percent thrust was 298 lbf-sec. Time from cutoff signal to 10 percent thrust was 0.2 seconds which is within the revised specification limit of 0.500 seconds (Reference 11).

## 8. APS CHAMBER PRESSURE EXCURSION

Postflight examination of the APS chamber pressure data (measurement GP2010P) revealed a rapid increase in pressure at 175:34:36.6 (hr:min:sec) AET, approximately 159 seconds after APS ignition. The chamber pressure increased from approximately 126 psia to 135 psia. During the next 10 seconds, the pressure measurement indicated a gradual decrease to approximately 127 psia. At 175:34:36.9 AET the measurement indicated another increase of approximately 6 to 8 psi. Following the second increase, the chamber pressure again decreased to the nominal level. Figure 13 shows the chamber pressure measurement data during the pressure fluctuations. During these times there was no indication of a pressure increase from either of the engine interface pressure measurements (GP1501P and GP1503P) or from the helium regulator outlet pressure measurements (GP0018P and GP0025P). To determine if the indicated pressure excursions were real, vehicle velocity data were examined for evidence of a corresponding change in engine thrust. In addition, several other key engine parameters (throat area, interface pressure, and C*) were also studied to determine if there were any changes in these parameters which corresponded to the chamber pressure increases.

The Primary Guidance and Navigation System (PGNS) velocity data were used to determine vehicle velocity changes ($\Delta V$) during the period of chamber pressure fluctuations. The $\Delta V$ for nominal APS propellant flow rates and thrust was determined for a 10 second interval. The RCS contribution to vehicle velocity increase was estimated using RCS on-time bi-level data. The total estimated $\Delta V$ agreed well with the PGNS data.

Next, using a combination of the partial derivatives generated by the PAP and the APS nonlinear on line (Time Share System) program, effects on $\Delta V$ due to changes in interface pressures and throat area commensurate with the observed shift in chamber pressure were investigated. It was determined that an increase of 18 psi (10.6 percent) in both oxidizer and fuel interface pressures would produce a 10 psi increase in chamber pressure and result in 5 ft/sec greater $\Delta V$ than in the nominal case. In addition, both the engine thrust and flow rate would be increased by over 8 percent. As stated above, no increases in interface pressures were observed in the flight data. A decrease in throat area sufficient to yield the observed chamber pressure shift would result in a reduction of engine thrust and flow rates as well as a 4 ft/sec decrease in $\Delta V$ for the 10-second interval. Figure 14 shows the PGNS $\Delta V$ data resolved and summed over 10-second intervals from approximately 50 seconds before and 50 seconds after the chamber pressure excursions. No unusual deviations in the velocity gain are apparent.

A similar analysis was made to determine what the acceleration history would look like if the chamber pressure did indeed increase as shown in Figure 13. Figure 15 shows the calculated acceleration history assuming an interface driven chamber pressure increase. Figure 16 shows the result of assuming a throat erosion driven chamber pressure increase.

It should be noted that the determination of the effects of a throat area change was approximate. The throat area required to produce the 10 psi chamber pressure increase resulted in a ratio of initial throat area to required (to produce the 10 psi shift) throat area that is beyond the range of the Rocketdyne APS engine characterization. Decreasing the throat area,

in general, increases the APS specific impulse. However, since the decrease in question is beyond the range of the engine characterization the magnitude of such a specific impulse increase was uncertain. Because of this, a conservative estimate of the increase was made using a partial derivative calculated in PAP. This approach yields a high side specific impulse estimation which would result in a smaller $\Delta V$ decrease.

One additional mechanism that might have resulted in a chamber pressure shift was a change in the C* efficiency of the engine. The theoretical C* for the APS engine at 1.6 mixture ratio is 5969.3 ft/sec. The nominal C* for the engine is 5748.4 ft/sec, an efficiency of 96.3 percent. If the actual engine C* were equal to the theoretical value, a chamber pressure increase of slightly less than 2 psi would result.

It is concluded that the chamber pressure shift seen in the flight data does not represent a real chamber pressure increase that would result in engine flow rate and thrust changes because there is no indication of such changes in either engine interface pressure data or in vehicle velocity change data. It is, therefore, suspected that the pressure excursions were due to an anomaly in the chamber pressure instrumentation.

# 9. CONCLUSIONS

The LM-11 APS flight reconstruction showed the APS performance to be satisfactory. No APS malfunctions or anomalies were noted.

## REFERENCES


1. NASA Document, MSC-07230, "Apollo 16 Mission Report," August 1972.

2. North American Rockwell Corporation Document No. PAR 8114-4102, "Lunar Module Ascent Engine Performance Characterization," T. A. Clemmer, 10 July 1968.

3. Rocketdyne Engine Log Book, "Acceptance Test Data Package for Rocket Engine Assembly - Ascent LM - Part No. RS000580-001-04, Serial No. 0013," 8 July 1969.

4. Boeing Report D2-118346-1, "Computer Program Manual Ascent Propulsion Subsystem Mixture Ratio by the Center of Mass Method," 28 August 1970.

5. TRW IOC 71.6522.1-14, "Apollo 16 Postflight Mass Properties," C. A. Anderson to B. R. Ellison, 26 May 1972.

6. NASA Memorandum EP-23-10-69, from EP2/Head Development Section to EP2/ Chief, Primary Propulsion Branch, "Propellant Densities ($N_2O_4$ and A-50)," 18 February 1969.

7. Spacecraft Operational Data Book, SNA-8-D-027 (III), Rev. 3, Vol. III, Amendment 124, 6 April 1972.

8. TRW Report 17618-H146-R0-00, "Apollo 14/LM-8 Ascent Propulsion System Final Flight Evaluation," September 1971.

9. TRW IOC 71.4915.2.47, "Ascent Propulsion System (APS) Characterization," W. Griffin to E-99 File, 2 November 1971.

10. TRW Report 20029-H001-R0-00, "Apollo Mission J2/LM-11/APS Preflight Performance Report," November 1971.

11. LTX-965-219, "P.O. 6-20900-C, LM Ascent Engine, LVC 275-0050051A," 2 July 1969.

TABLE 1. LM-11/APS ENGINE AND FEED SYSTEM PHYSICAL CHARACTERISTICS

| | |
|---|---|
| Engine[(a)] | |
| Engine No. | Rocketdyne S/N 0013C |
| Injector No. | Rocketdyne S/N4097735 |
| Initial Chamber Throat Area ($in^2$) | 16.44 |
| Nozzle Exit Area ($in^2$) | 749.59 |
| Initial Expansion Ratio | 45.58 |
| Injector Resistance ($lbf\text{-}sec^2/lbm\text{-}ft^5$)@ time zero and 70°F | |
| Oxidizer | 12312.0 |
| Fuel | 19880.6 |
| Feed System | |
| Total Volume (Pressurized, Check Valves to engine interface)($ft^3$)[(b)] | |
| Oxidizer | 36.95 |
| Fuel | 37.00 |
| Resistance, Tank Bottom to Engine Interface ($lbf\text{-}sec^2/lbm\text{-}ft^5$) at 70°F[(c)] | |
| Oxidizer | 2633.76 |
| Fuel | 4078.08 |

(a) Rocketdyne Log Book, "Acceptance Test Data Package for Rocket Engine Assembly-Ascent LM-Part No. RS000580-001-04, Serial No. 0013," 8 July 1969.

(b) NASA Memorandum EP23-46-69, "Propellant Load Parameters for the DPS and APS of LM-5 through LM-9 and the Estimated Parameters for LM-10 and Subsequent," from EP/Chief, Propulsion and Power Division to PD/Chief, Systems Engineering Division.

(c) GAC Memorandum LMO-271-194, "A/S Hydraulic Resistance LM-8 through LM-12 as per NASA/MSC Data Request Under CCA #467," T. Laterra, 26 October 1970.

TABLE 2. LM-11 APS PROPELLANT AND HELIUM CONSUMPTION

Propellant from APS Tanks

| | Oxidizer | Fuel |
|---|---|---|
| Propellant Loaded - lbm | 3224.7 | 2017.8 |
| Transferred from RCS tank during coast - lbm | 44.0 | 16.0 |
| Total @ Lunar Lift-off - lbm | 3268.7 | 2033.8 |
| Consumption during Lunar Lift-off Burn - lbm | | |
| APS | 2990.3 | 1875.3 |
| RCS | 51.3 | 25.7 |
| Total | 3041.6 | 1901.0 |
| Propellant Remaining - lbm | 227.1 | 132.8 |
| Consumed During TPI Burn - lbm | 18.8 | 11.2 |
| Propellant Remaining - lbm | 208.3 | 121.6 |

APS Helium Tank Usage

| | |
|---|---|
| Loaded - lbm | 13.2 |
| Consumed - lbm | 8.4 |
| Remaining - lbm | 4.8 |

TABLE 3. FLIGHT DATA USED IN STEADY-STATE ANALYSIS

| Measurement Number | Description | Range | Sample Rate Sample/sec |
|---|---|---|---|
| GP2010P | Pressure, Thrust Chamber | 0-150 psia | 200 |
| GP1503P | Pressure, Engine Oxidizer Interface | 0-250 psia | 1 |
| GP1501P | Pressure, Engine Fuel Interface | 0-250 psia | 1 |
| GP0025P | Pressure, Regulator Outlet Manifold | 0-300 psia | 1 |
| GP0018P | Pressure Regulator Outlet Manifold | 0-300 psia | 1 |
| GP1218T | Temperature, Oxidizer Tank Bulk | 20-120°F | 1 |
| GP0718T | Temperature, Fuel Tank Bulk | 20-120°F | 1 |
| GH1260X | Ascent Engine On/Off | Off-On | 50 |
| GP0001P | Pressure, Helium Supply Tank No. 1 | 0-4000 | 1 |
| GP0002P | Pressure, Helium Supply Tank No. 2 | 0-4000 | 1 |
| GP0041P | Pressure, Helium Supply Tank No. 1 | 0-4000 | 10 |
| GP0042P | Pressure, Helium Supply Tank No. 2 | 0-4000 | 10 |
| CG0001X* | PGNS Downlink Data | Digital Code | 50 |

*Acceleration determined from PIPA data.

TABLE 4. LM-11 APS STEADY-STATE PERFORMANCE

| PARAMETER | 20 sec After Ignition | | | 200 sec After Ignition | | | 390 sec After Ignition | | |
|---|---|---|---|---|---|---|---|---|---|
| | (a) Pred. | (b) Reconstructed | (c) Measured | (a) Pred. | (b) Reconstructed | (c) Measured | (a) Pred. | (b) Reconstructed | (c) Measured |
| Regulator Outlet Pressure, psia | 184. | --- | 183.8 | 184. | --- | 183.8 | 184. | --- | 182.0 |
| Oxidizer Bulk Temperature °F | 70.0 | --- | 68.8 | 69.7 | --- | 68.8 | 69.0 | --- | 68.8 |
| Fuel Bulk Temperature °F | 70.0 | --- | 70.8 | 69.9 | --- | 70.8 | 69.8 | --- | 70.8 |
| Oxidizer Interface Pressure, psia | 170.6 | 170.0 | 171.0 | 170.4 | 170.1 | 170.8 | 169.6 | 169.3 | 169.6 |
| Fuel Interface Pressure, psia | 170.2 | 170.8 | 170.3 | 170.2 | 170.5 | 170.0 | 169.5 | 169.6 | 169.0 |
| Engine Chamber Pressure, psia | 123.5 | 123.6 | 125.9 | 123.9 | 123.5 | 125.3 | 123.0 | 122.2 | 123.4 |
| Mixture Ratio | 1.601 | 1.593 | --- | 1.598 | 1.595 | --- | 1.594 | 1.593 | --- |
| Thrust, lbf | 3518 | 3547. | --- | 3495. | 3542. | --- | 3495. | 3544. | --- |
| Specific Impulse, sec | 309.7 | 312.0 | --- | 309.8 | 312.0 | --- | 309.1 | 311.1 | --- |

(a) Preflight prediction based on acceptance test data and assuming nominal system performance.
(b) Reconstruction minimum variance technique.
(c) Smoothed flight data without biases determined by postflight analysis.

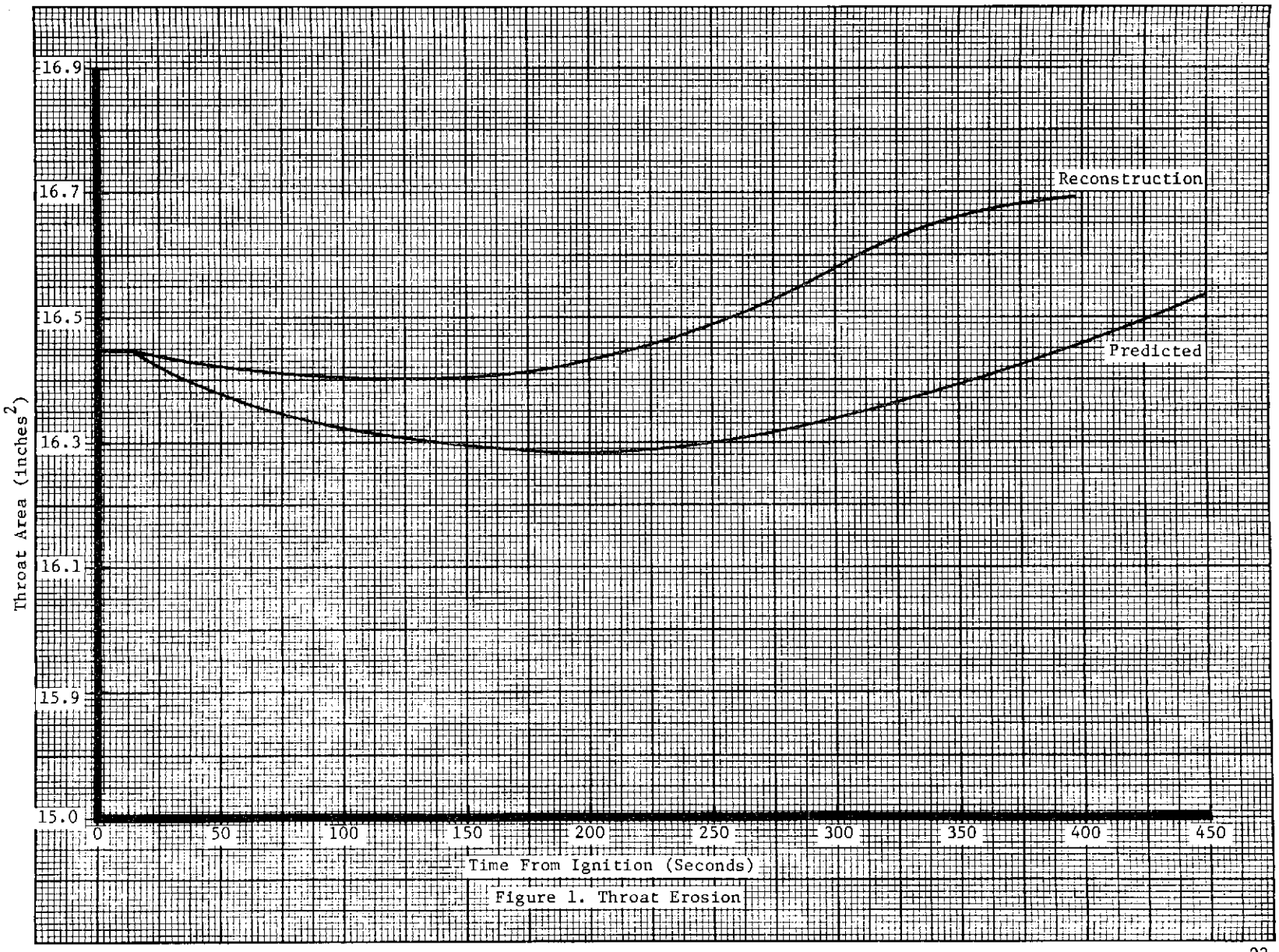


Figure 1. Throat Erosion

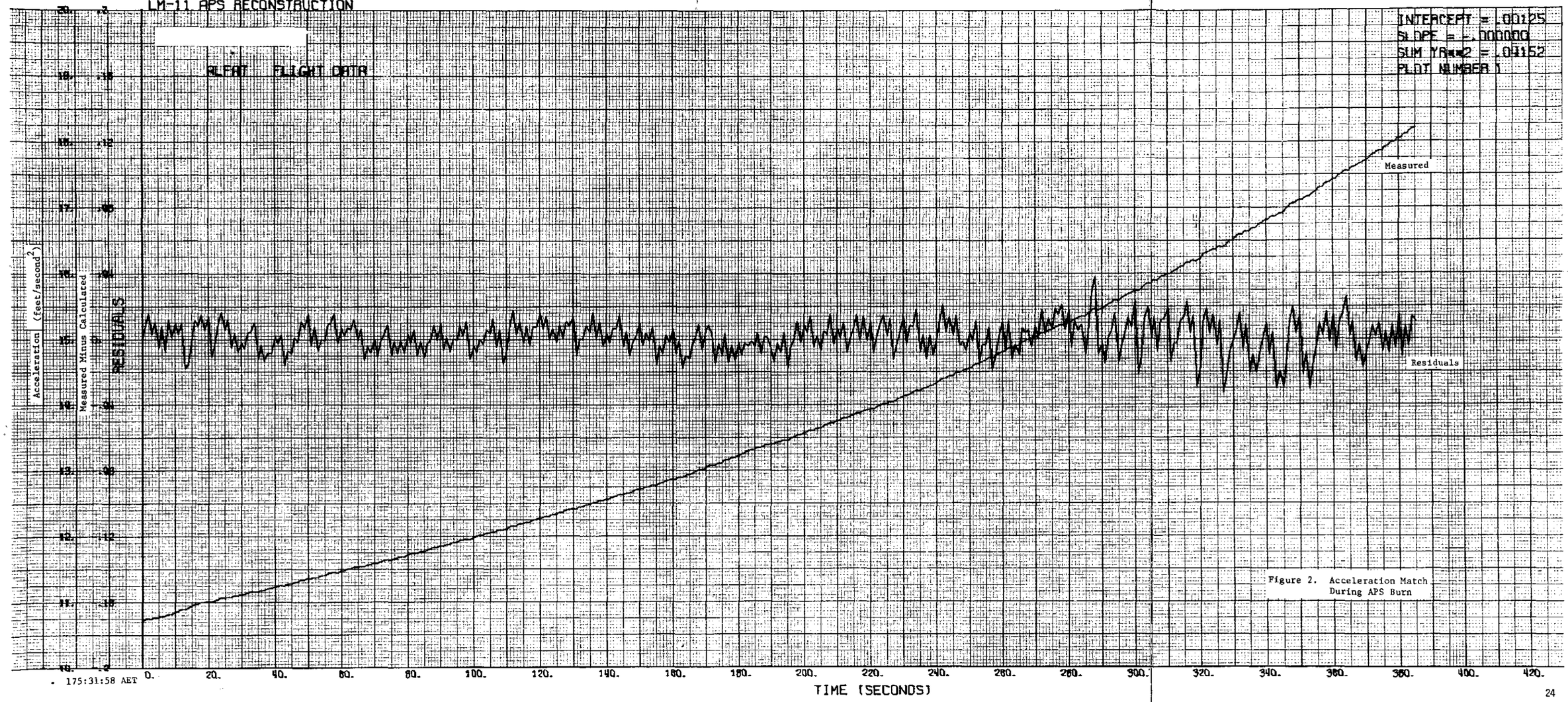


Figure 2. Acceleration Match During APS Burn



FOLDOUT FRAME 1

FOLDOUT FRAME 2

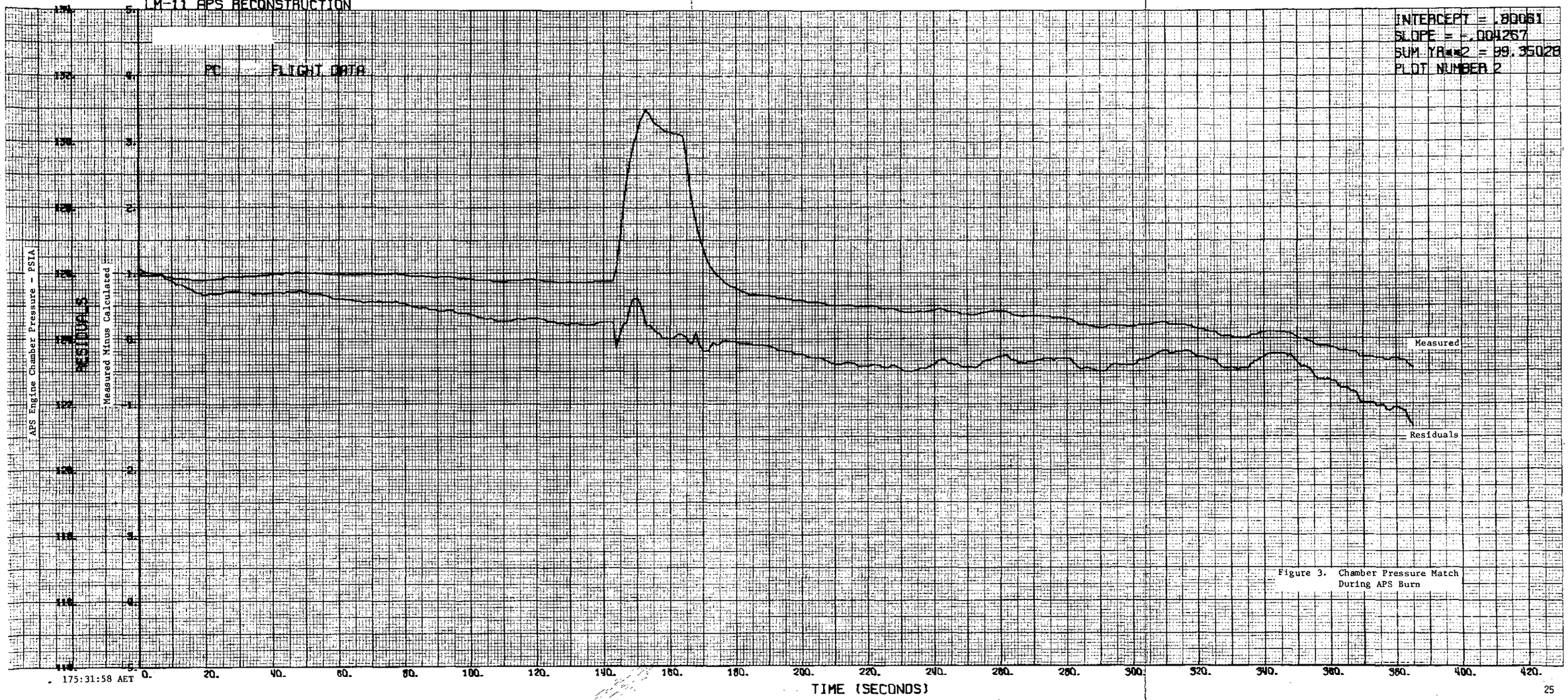


Figure 3. Chamber Pressure Match During APS Burn



FOLDOUT FRAME 1

FOLDOUT FRAME 2

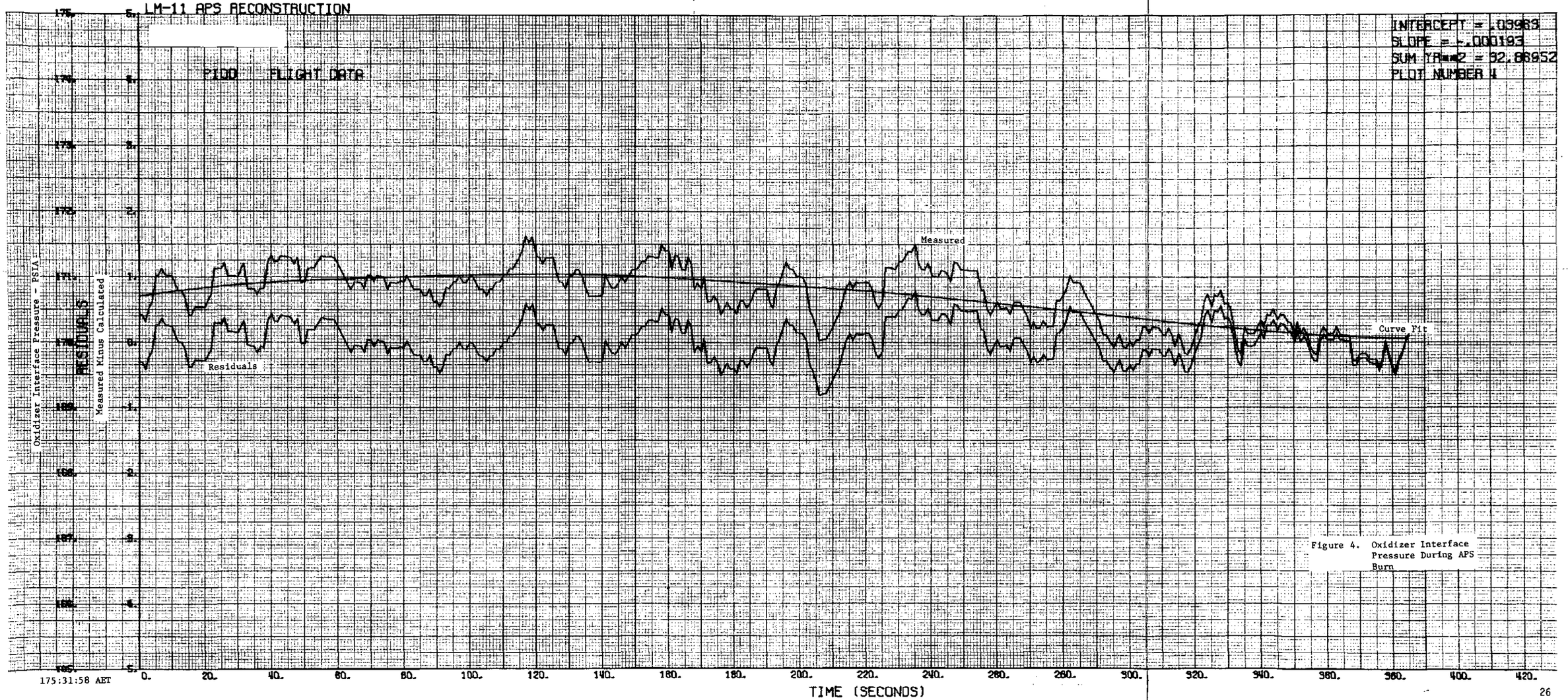


Figure 4. Oxidizer Interface Pressure During APS Burn



FOLDOUT FRAME 1

FOLDOUT FRAME 5

LM-11 APS RECONSTRUCTION

PIFO FLIGHT DATA

INTERCEPT = -.00193
SLOPE = -.000113
SUM YR**2 = 10.90313
PLOT NUMBER 5

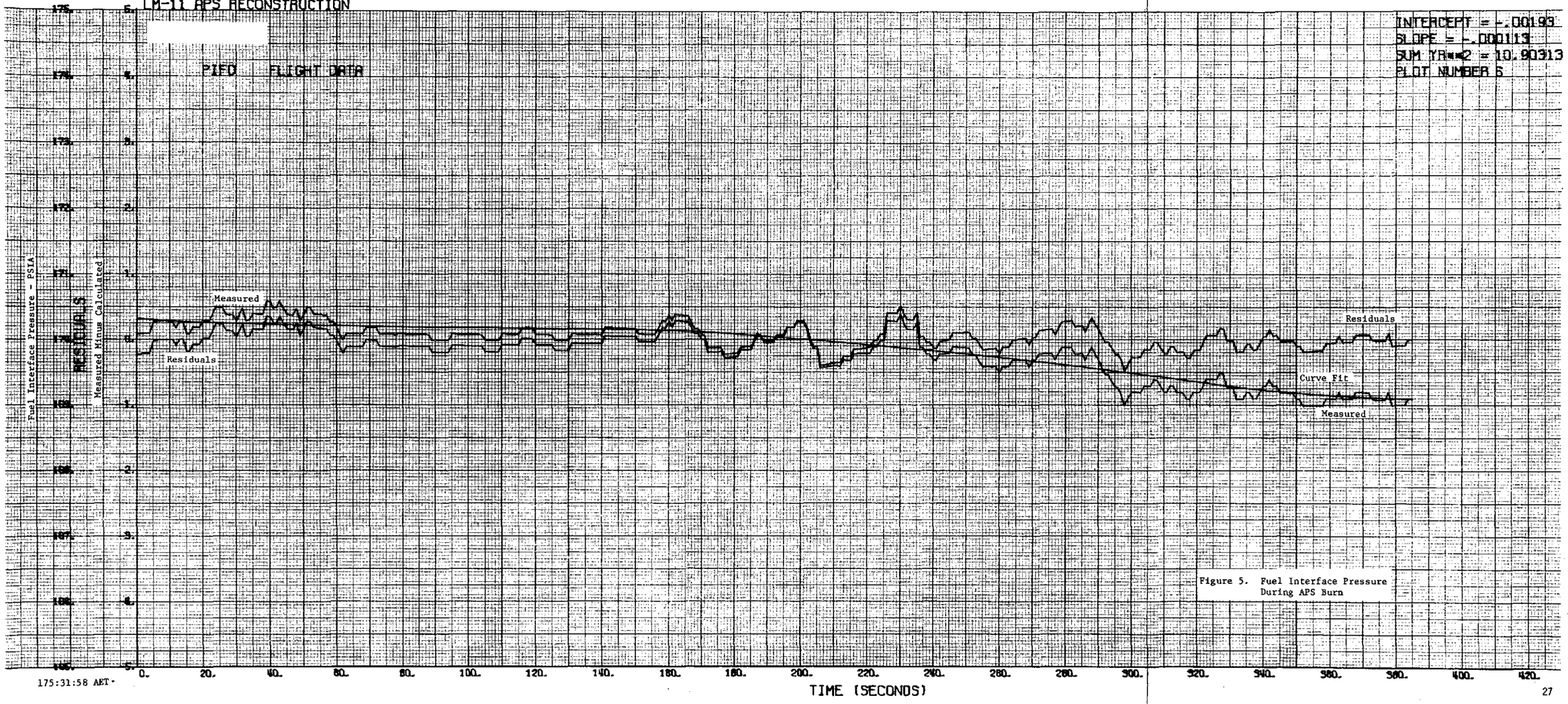


Figure 5. Fuel Interface Pressure During APS Burn



FOLDOUT FRAME 1

FOLDOUT FRAME 2

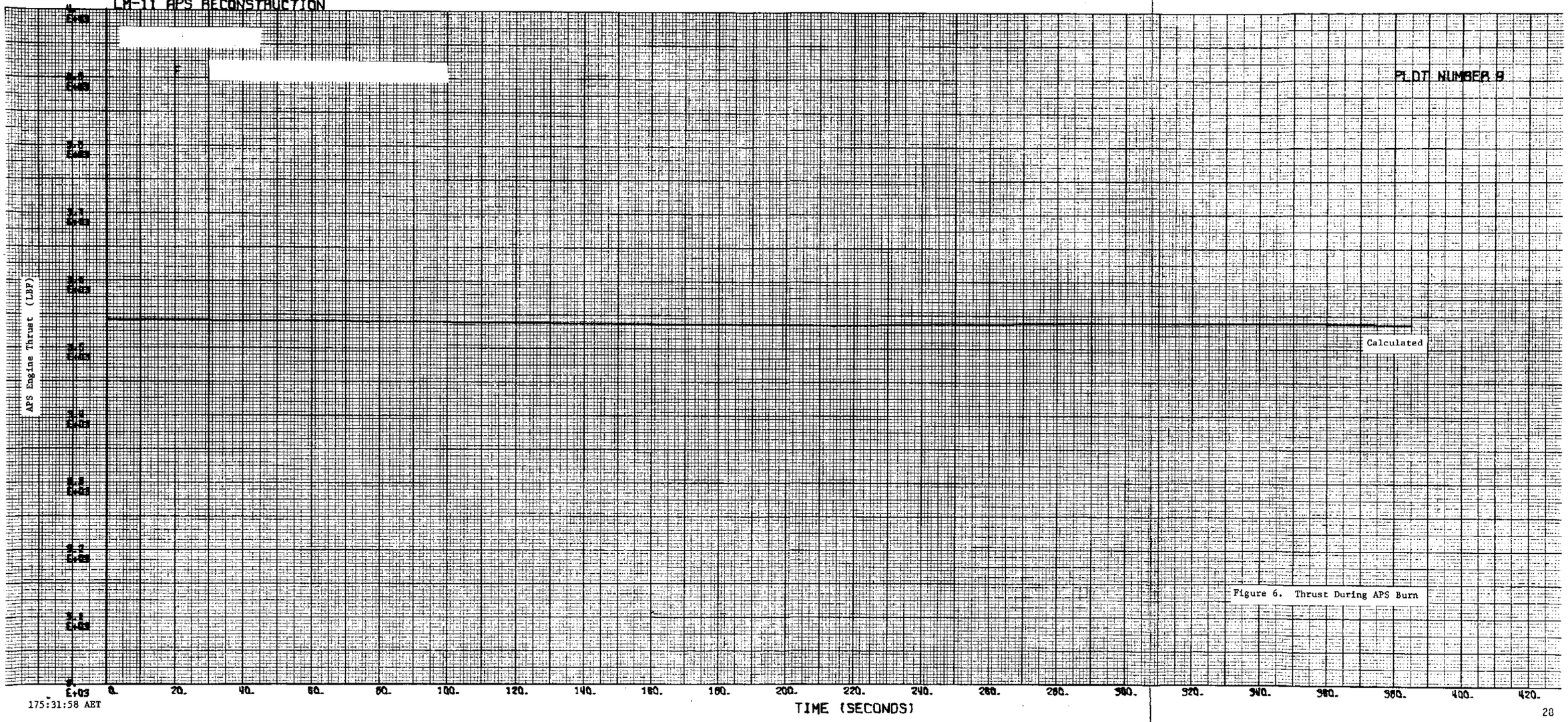


Figure 6. Thrust During APS Burn



FOLDOUT FRAME 1

FOLDOUT FRAME 2

LM-11 APS RECONSTRUCTION

ISP

PLOT NUMBER 12

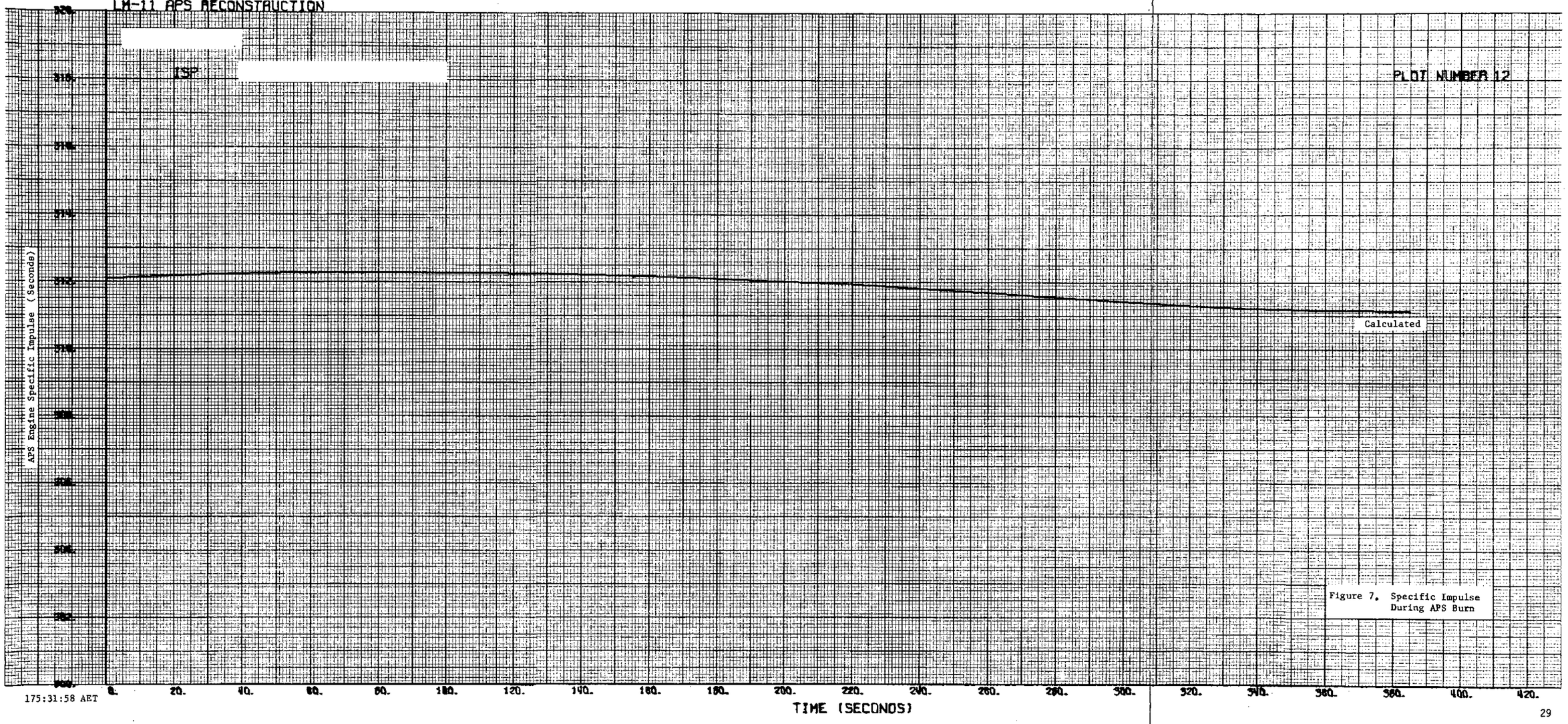


Figure 7. Specific Impulse During APS Burn

175:31:58 AET



FOLDOUT FRAME /

FOLDOUT FRAME 2

LM-11 APS RECONSTRUCTION

PLOT NUMBER 10

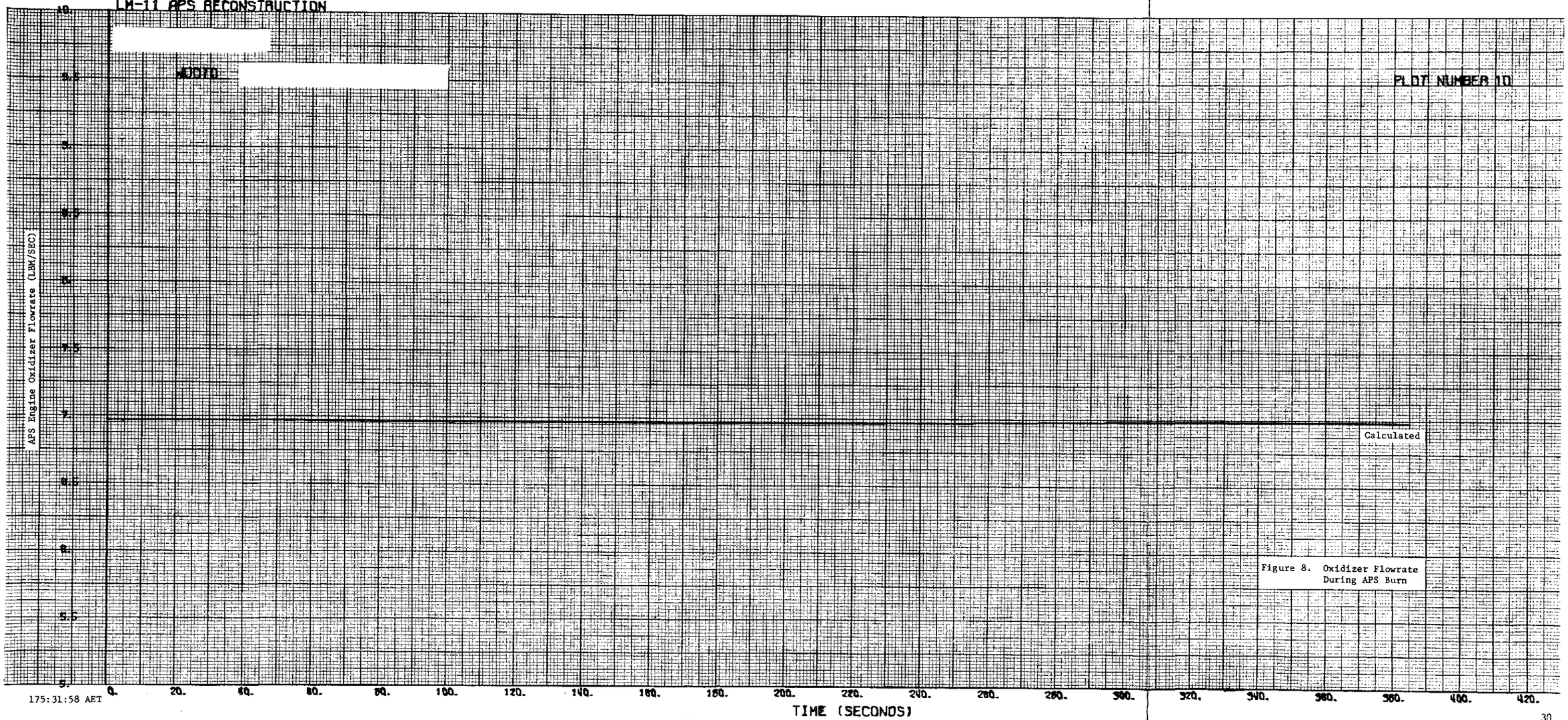


Figure 8. Oxidizer Flowrate During APS Burn



FOLDOUT FRAME 1

FOLDOUT FRAME 2

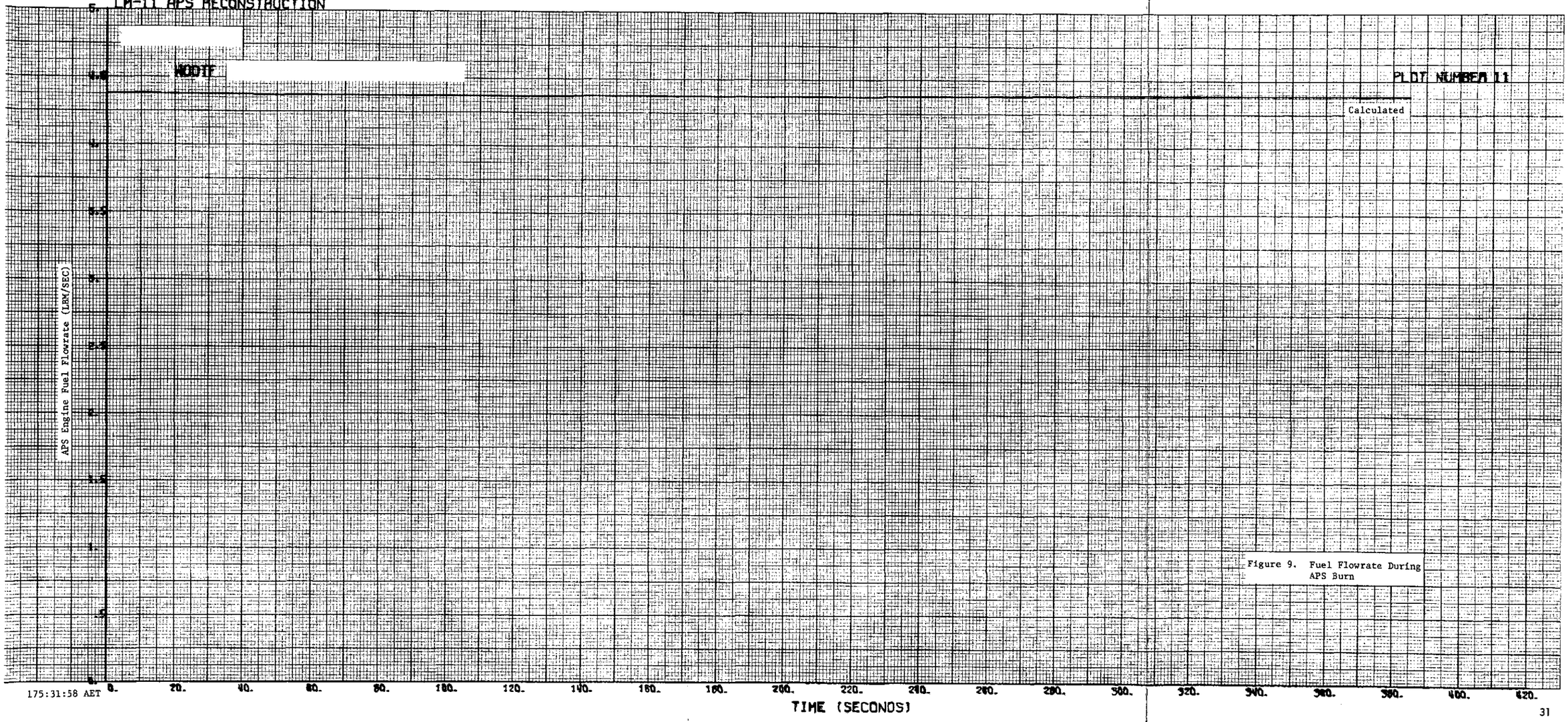


Figure 9. Fuel Flowrate During APS Burn



FOLDOUT FRAME 1

FOLDOUT FRAME 2

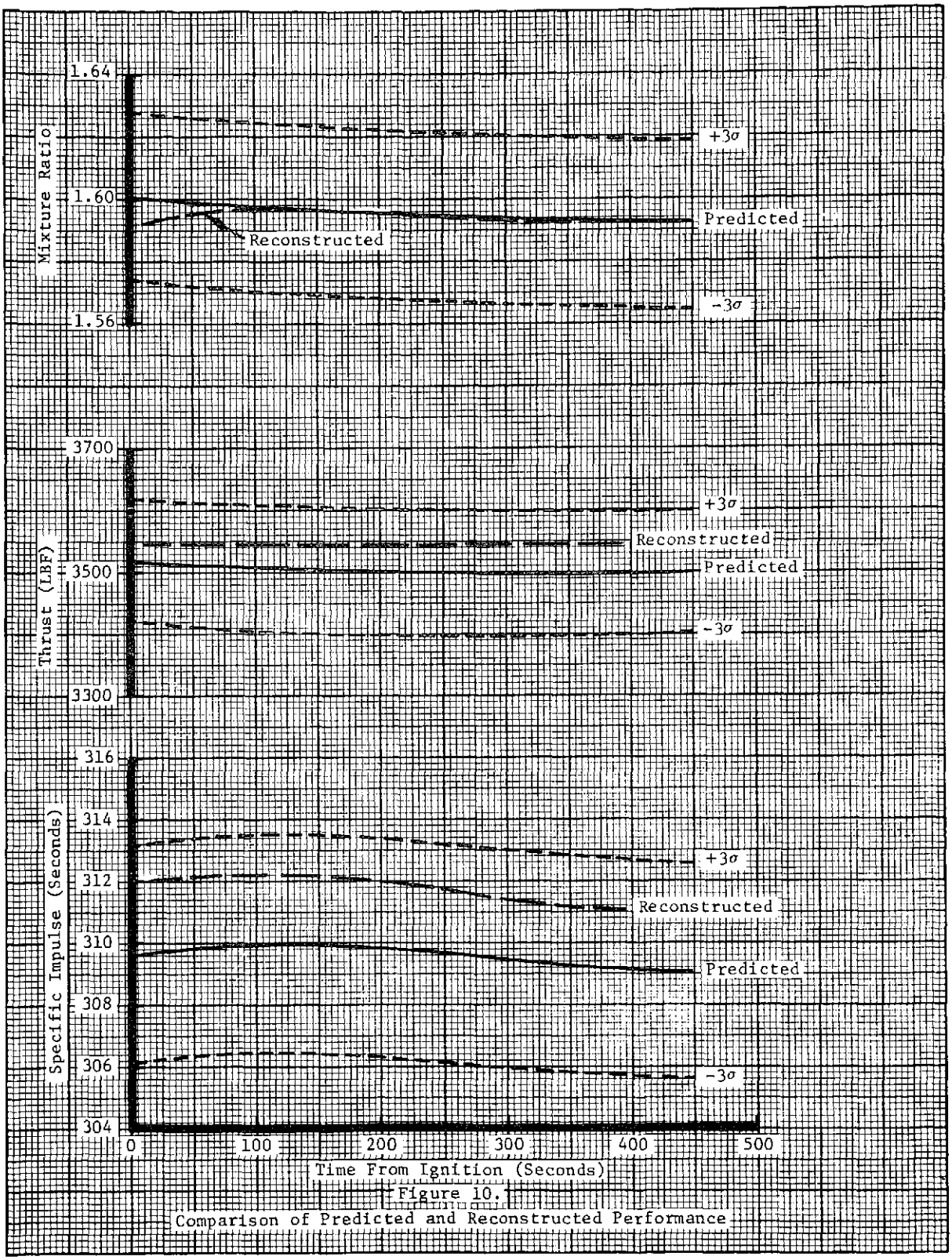


Figure 10.

Comparison of Predicted and Reconstructed Performance

APOLLO 16 SC113/LM11-APS-(RAW DATA)-ASCENT SD

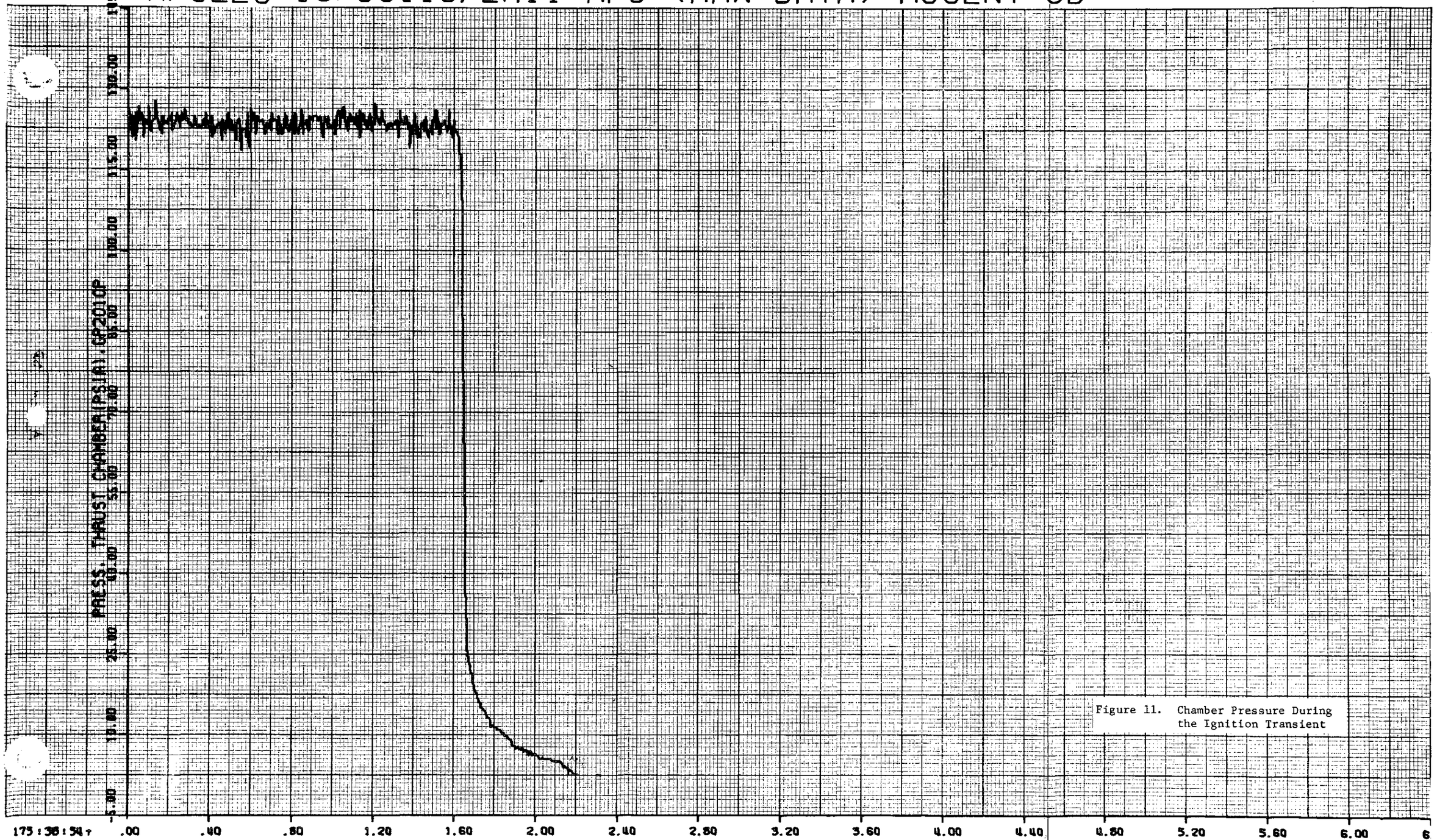


Figure 11. Chamber Pressure During the Ignition Transient



FOLDOUT FRAME 1

FOLDOUT FRAME 2

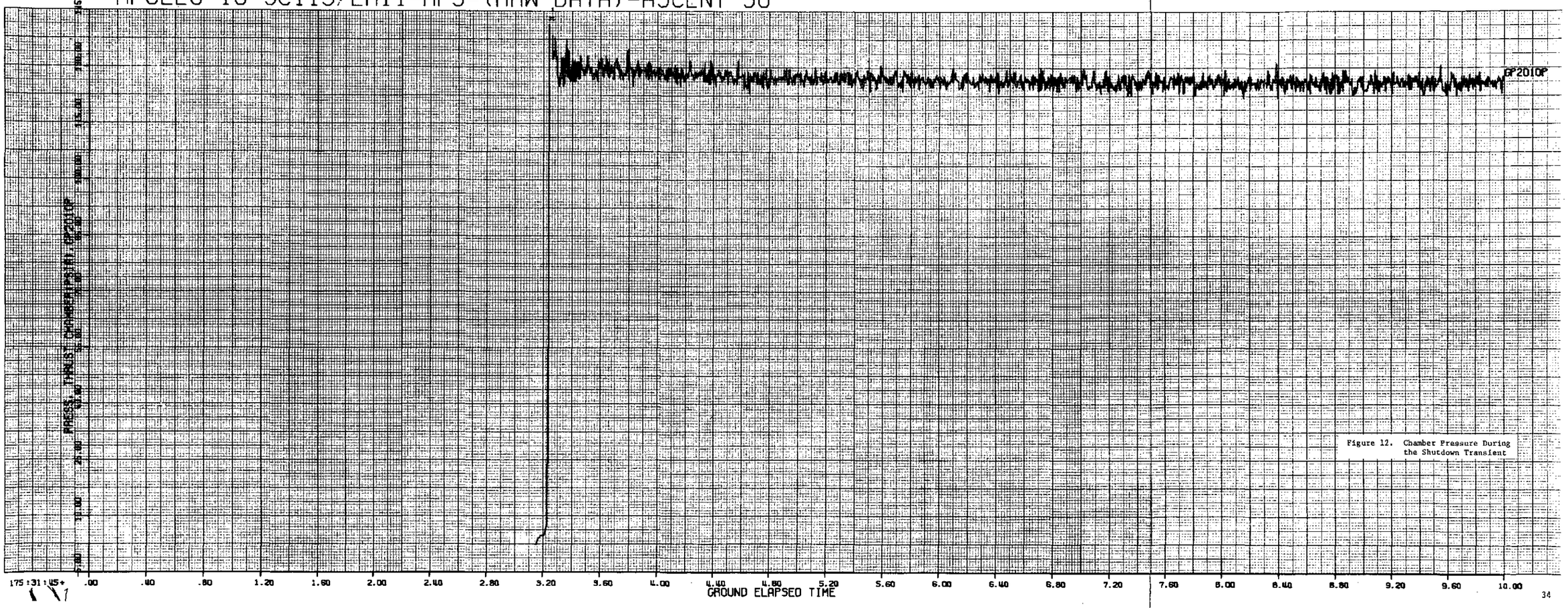


Figure 12. Chamber Pressure During the Shutdown Transient



FOLDOUT FRAME 1

FOLDOUT FRAME 2

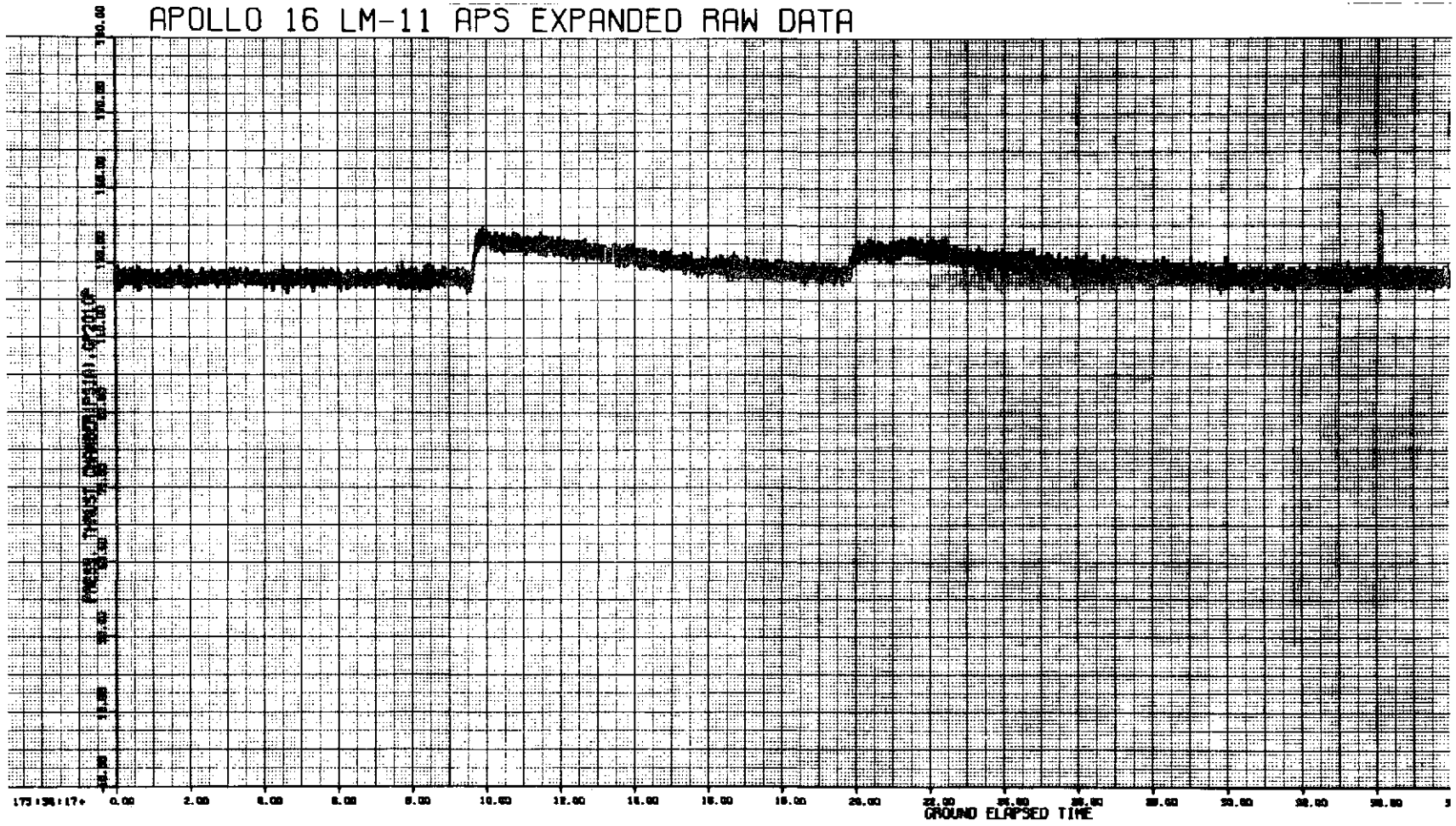


Figure 13.

Chamber Pressure Excursion

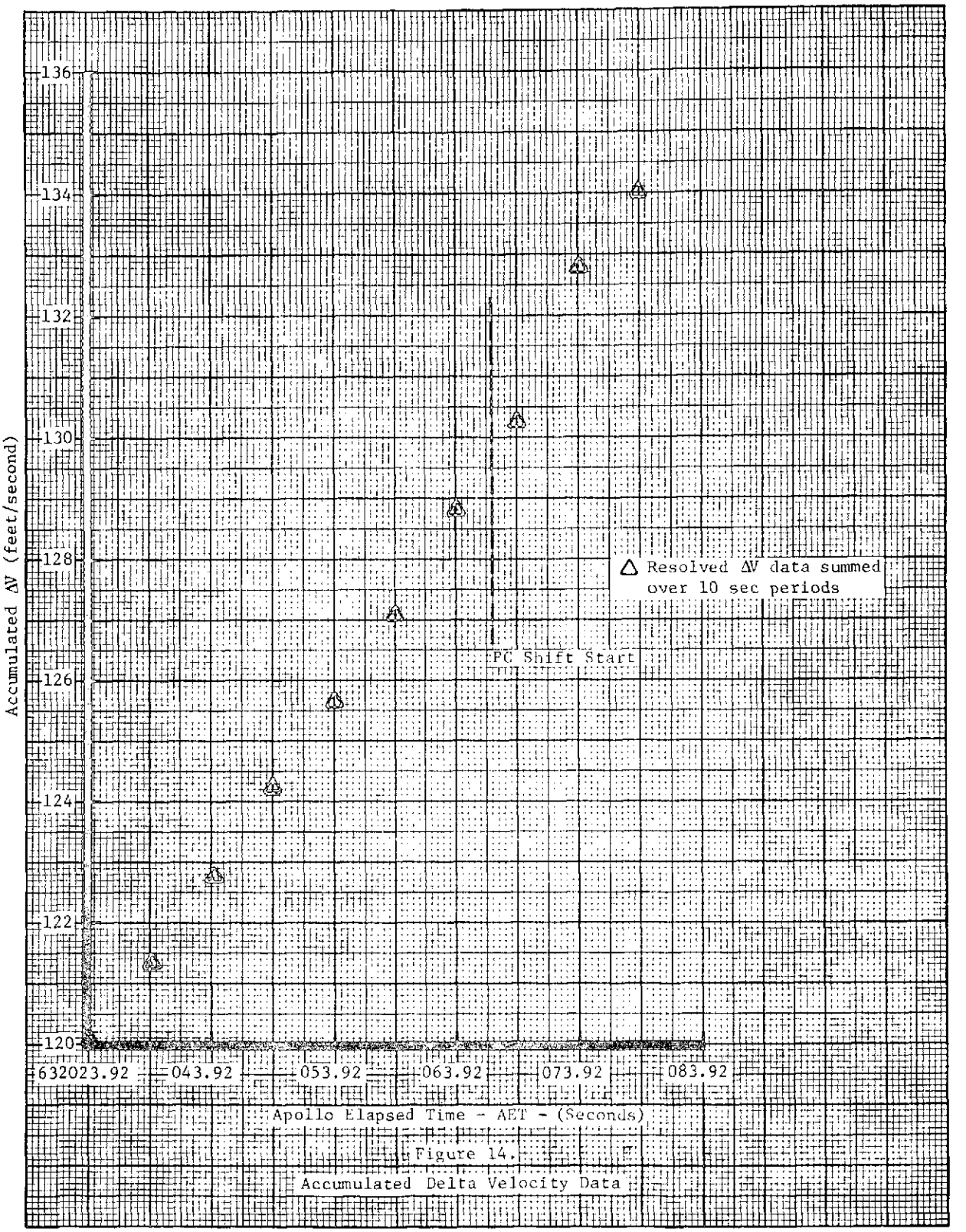


Figure 14.

Accumulated Delta Velocity Data

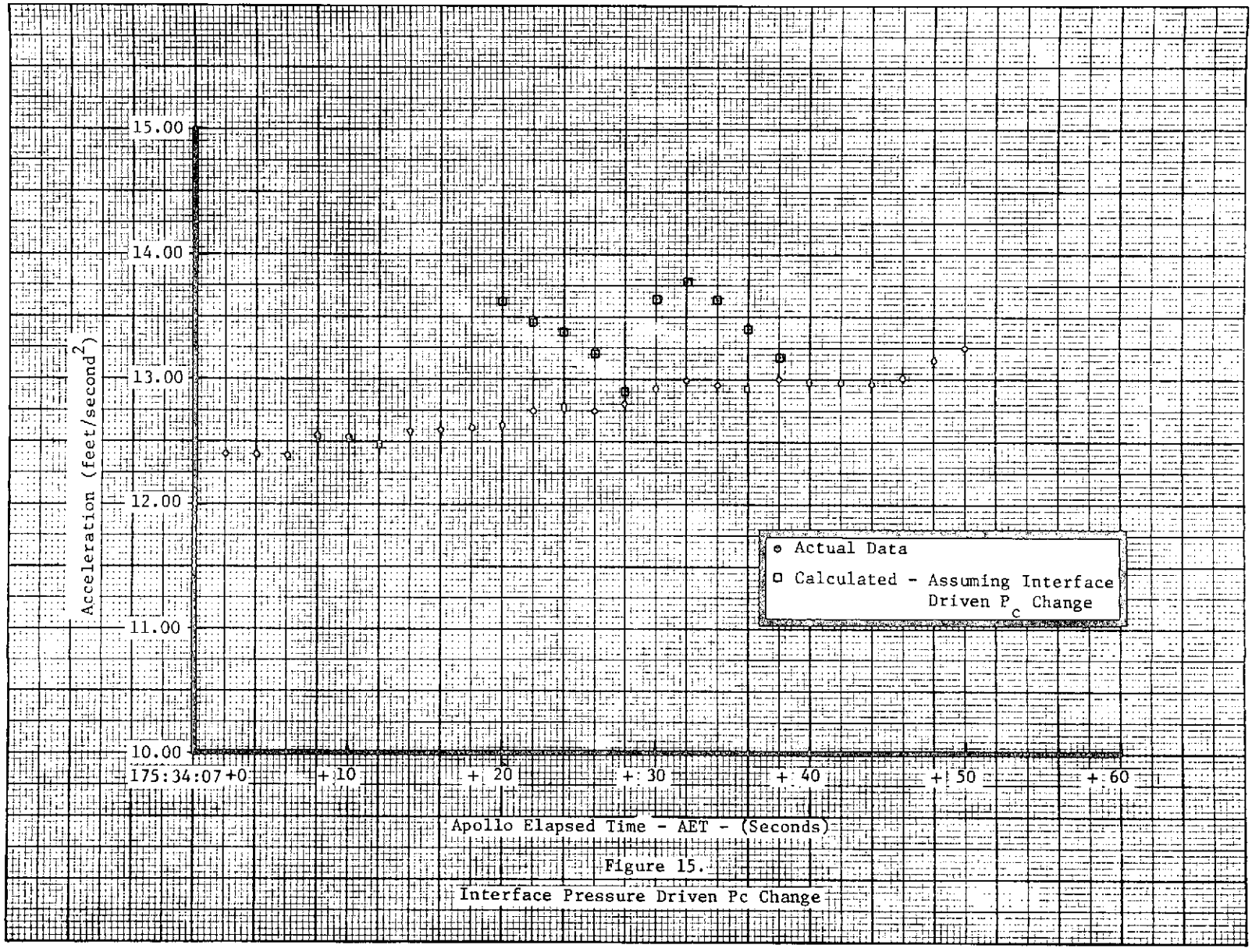


Figure 15.

Interface Pressure Driven Pc Change

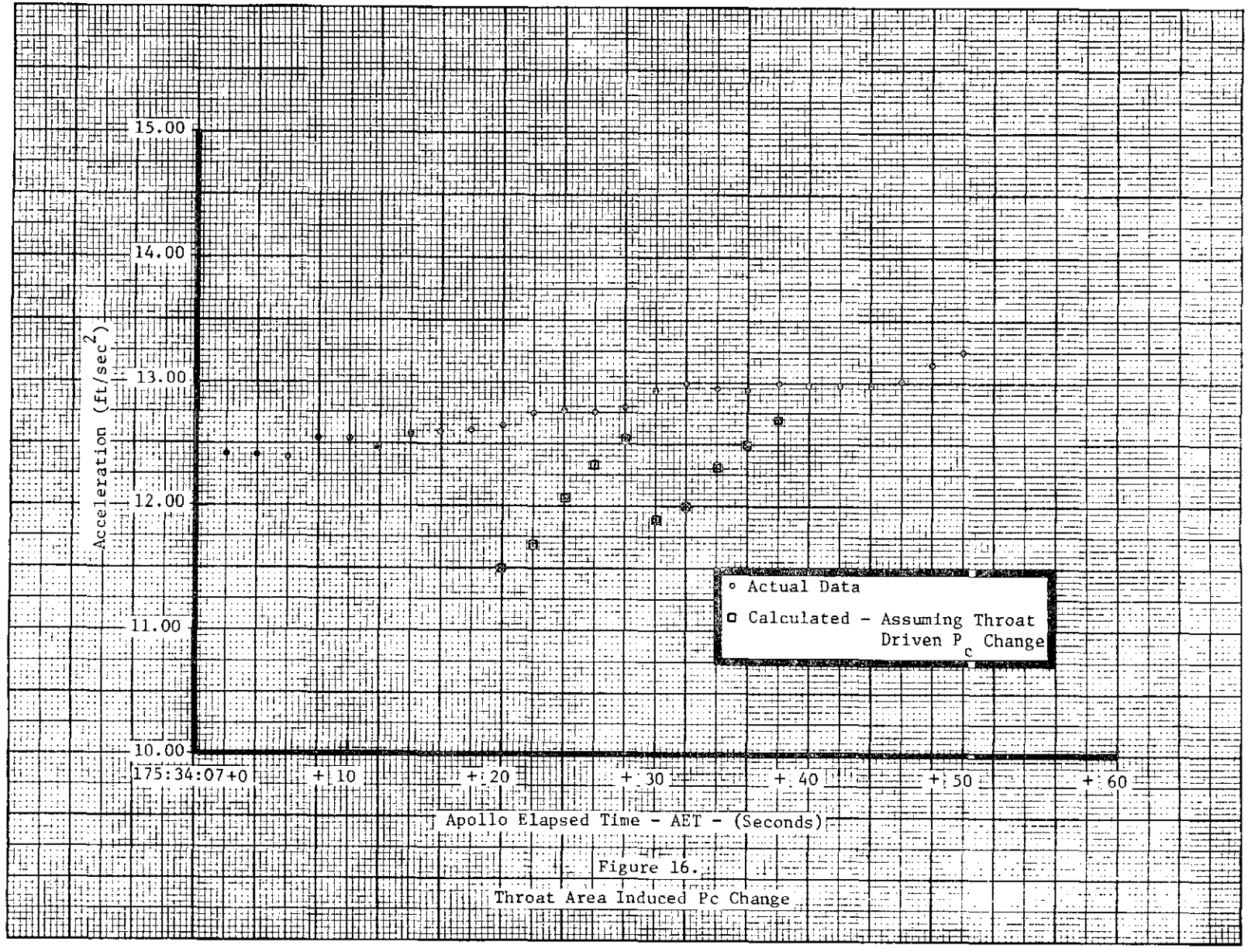


Figure 16.

Throat Area Induced Pc Change

APOLLO 16 SC113/LM11-APS-(RAW DATA)-ASCENT

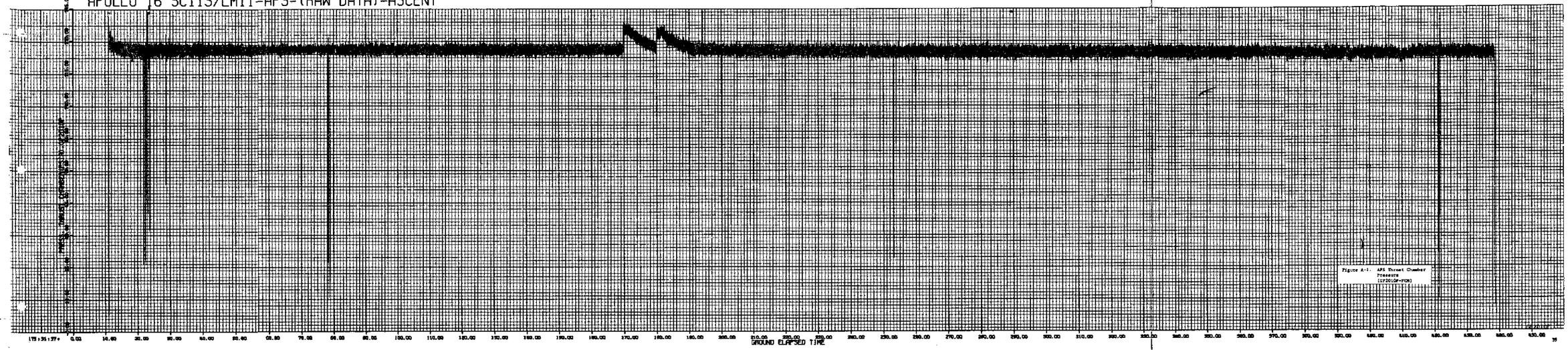


Figure A-1. APS Thrust Chamber Pressure (GP13COP-P2M)

APOLLO 16 SC113/LM11-APS-(RAW DATA)-ASCENT

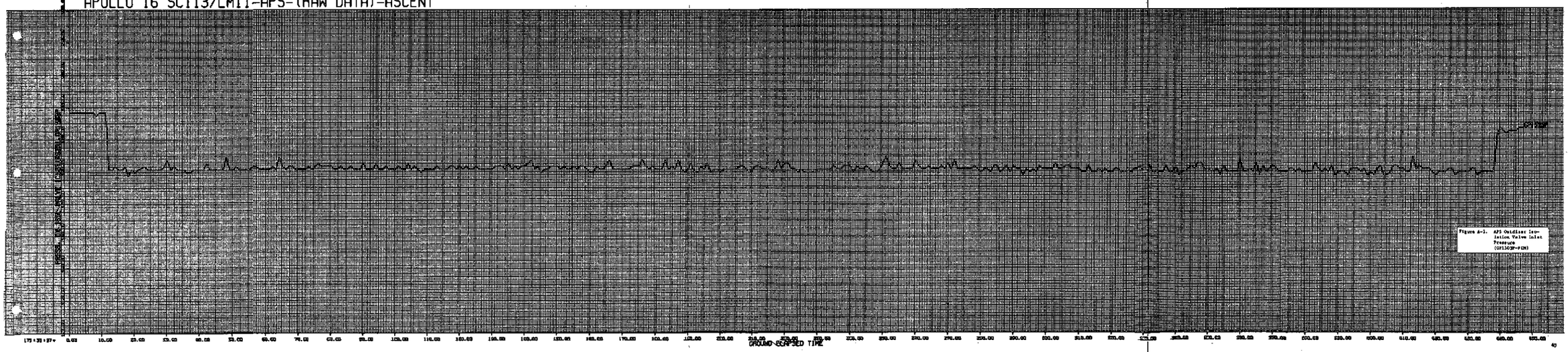


Figure A-2. APS Oxidizer Isolation Valve Inlet Pressure (GP13COP-P2M)

FOLDOUT FRAME 1

FOLDOUT FRAME 2

APOLLO 16-SC113/LM11-APS-(RAW DATA)-ASCENT

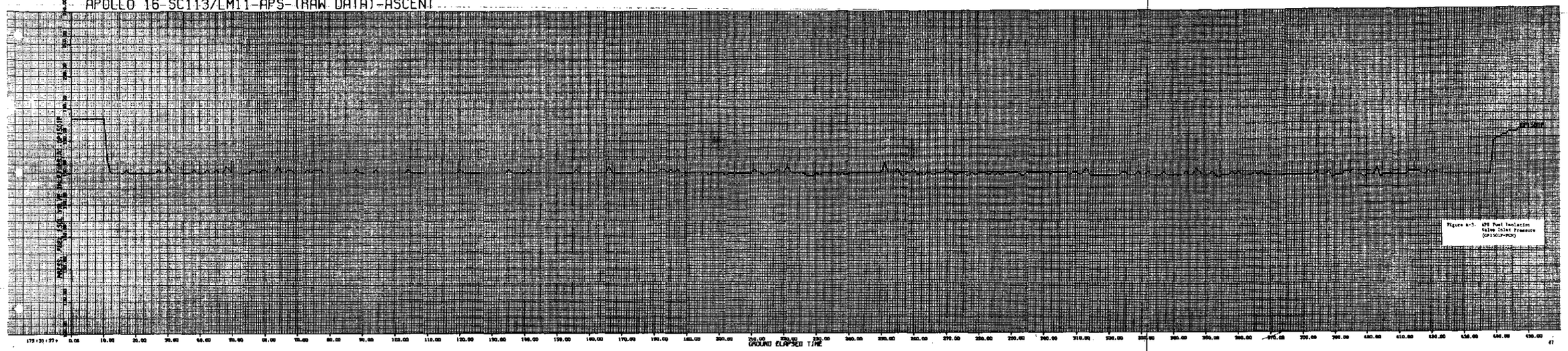


Figure A-3. APS Fuel Isolation Valve Inlet Pressure (GP150LP-PCM)



APOLLO 16 SC113/LM11-APS-(RAW DATA)-ASCENT

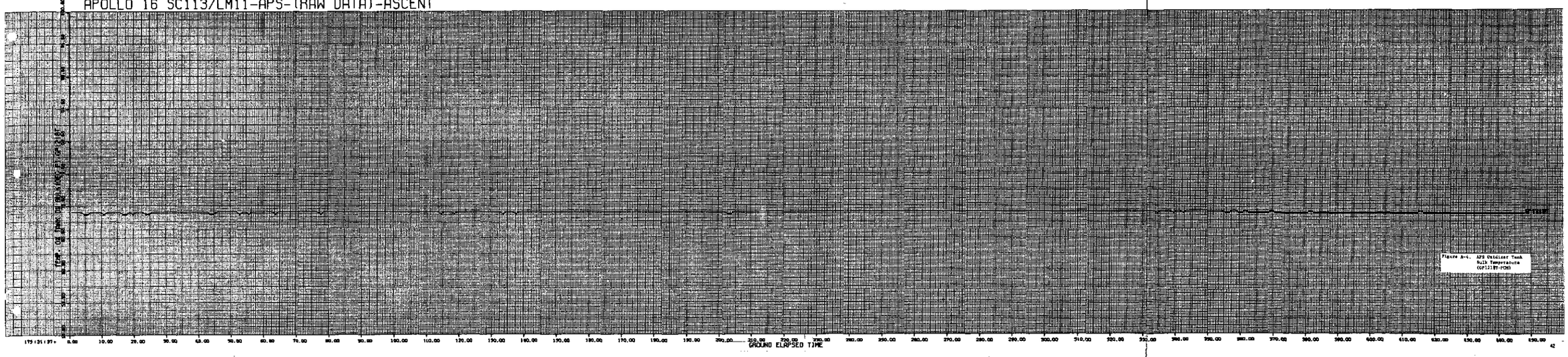


Figure A-4. APS Oxidizer Tank Bulk Temperature (GP121BT-PCM)



FOLDOUT FRAME 1

FOLDOUT FRAME 2

APOLLO 16 SC113/LM11-APS-(RAW DATA)-ASCENT

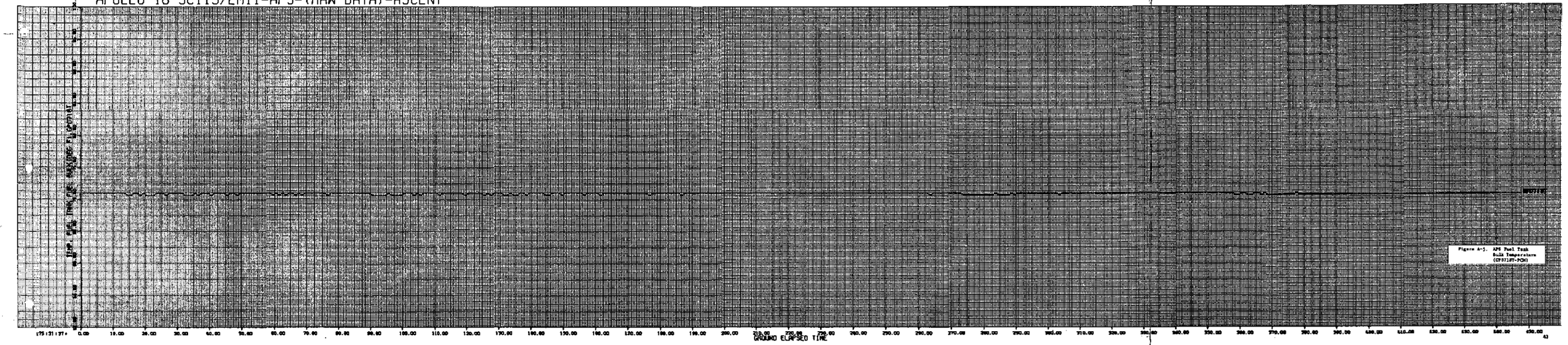


Figure A-1. APS Fuel Tank Bulk Temperature (CP9712T-POM)

APOLLO 16 SC113/LM11-APS-(RAW DATA)-ASCENT

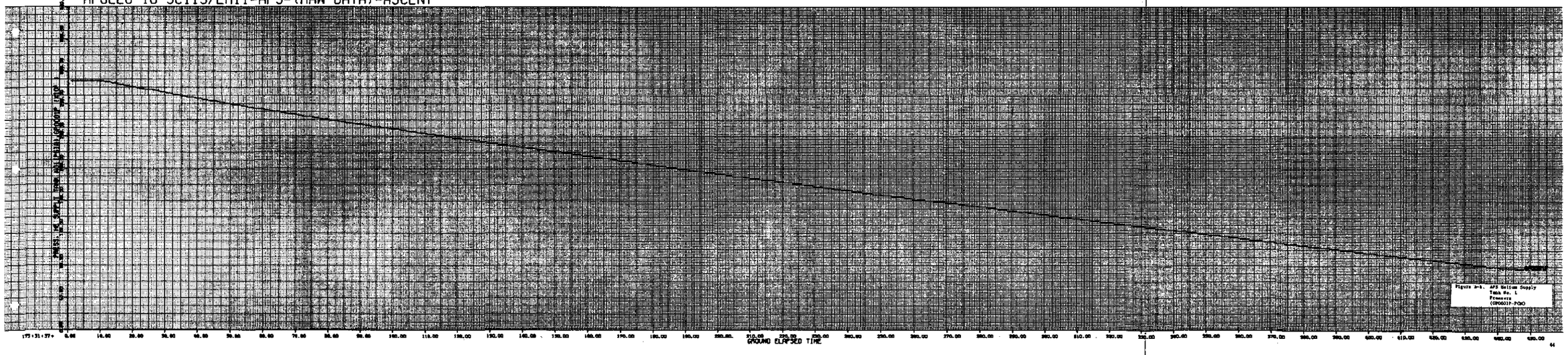


Figure A-2. APS Helium Supply Tank No. 1 Pressure (CP9003P-POM)

FOLDOUT FRAME 1

FOLDOUT FRAME 2

APOLLO 16 SC113/LM11-APS-(RAW DATA)-ASCENT

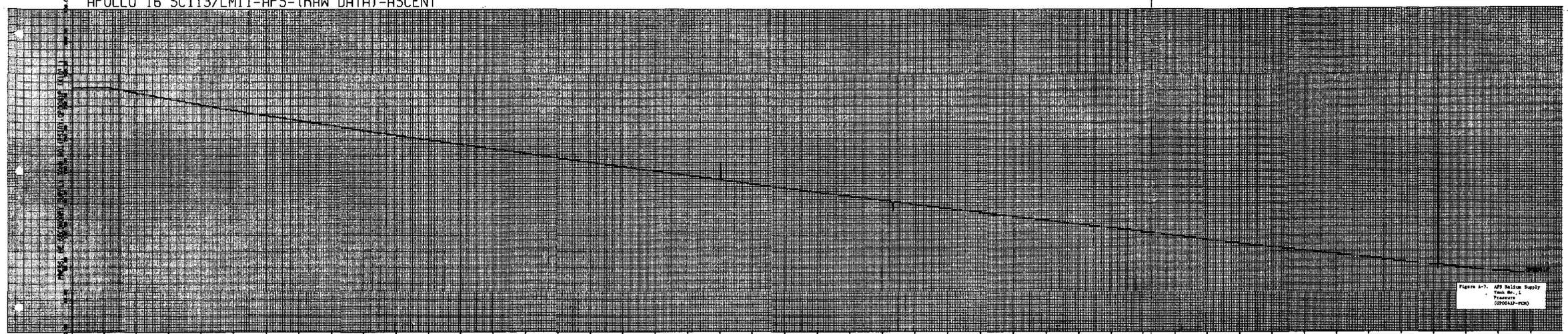


Figure A-7. APS Helium Supply Tank No. 1 Pressure (GP0004P-PCM)

45

APOLLO 16 SC113/LM11-APS-(RAW DATA)-ASCENT

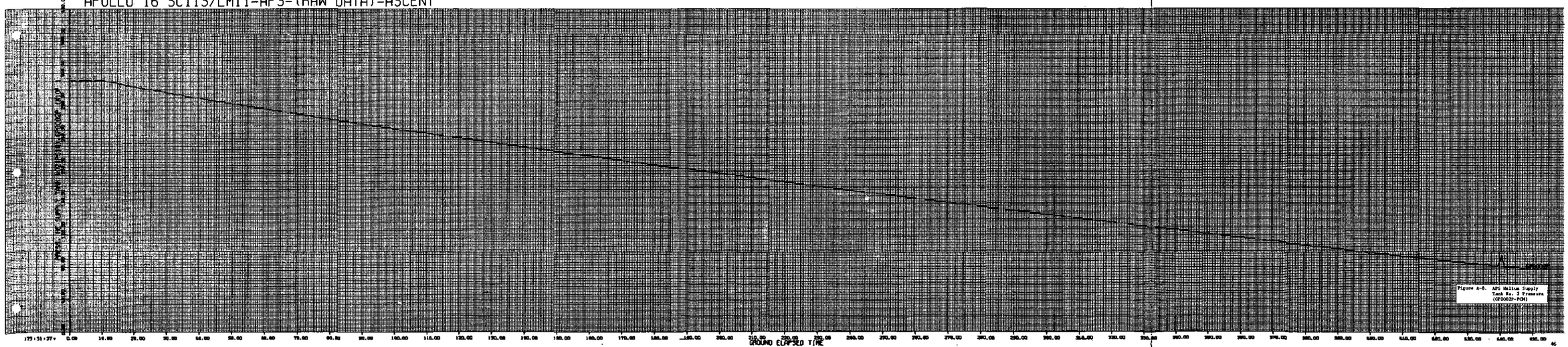


Figure A-8. APS Helium Supply Tank No. 2 Pressure (GP0002P-PCM)

46

FOLDOUT FRAME /

FOLDOUT FRAME 2

APOLLO 16 SC113/LM11-APS-(RAW DATA)-ASCENT

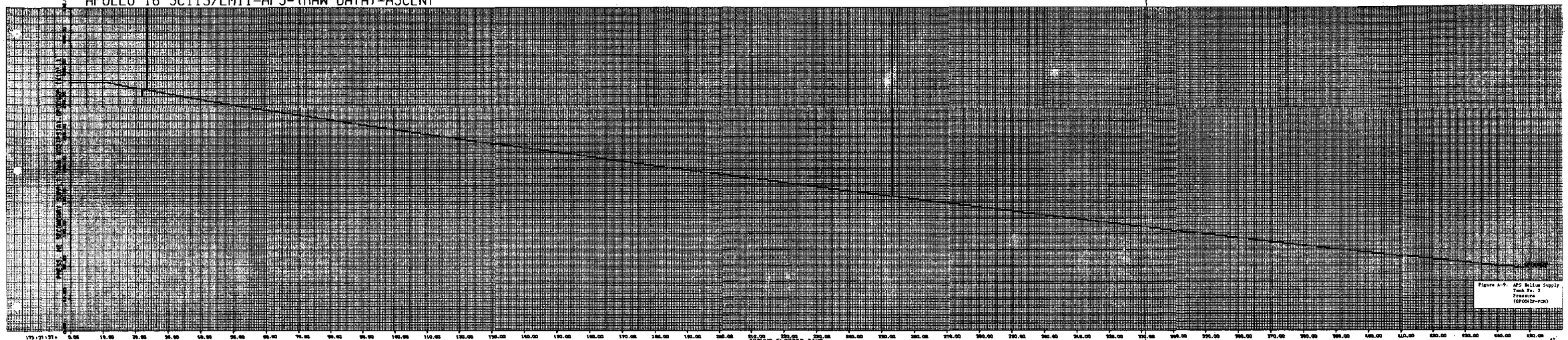


Figure A-9. APS Helium Supply Tank No. 2 Pressure (CP00629-PCM)

APOLLO 16 SC113/LM11-APS-(RAW DATA)-ASCENT

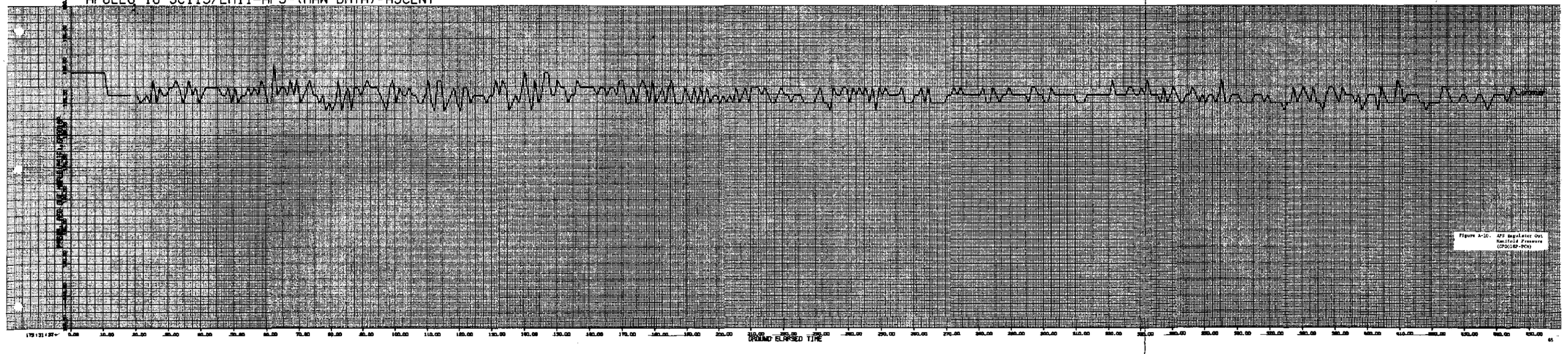


Figure A-10. APS Regulator Out Manifold Pressure (CP00582-PCM)

FOLDOUT FRAME 1

FOLDOUT FRAME 2

APOLLO 16 SC113/LM11-APS-(RAW DATA)-ASCENT

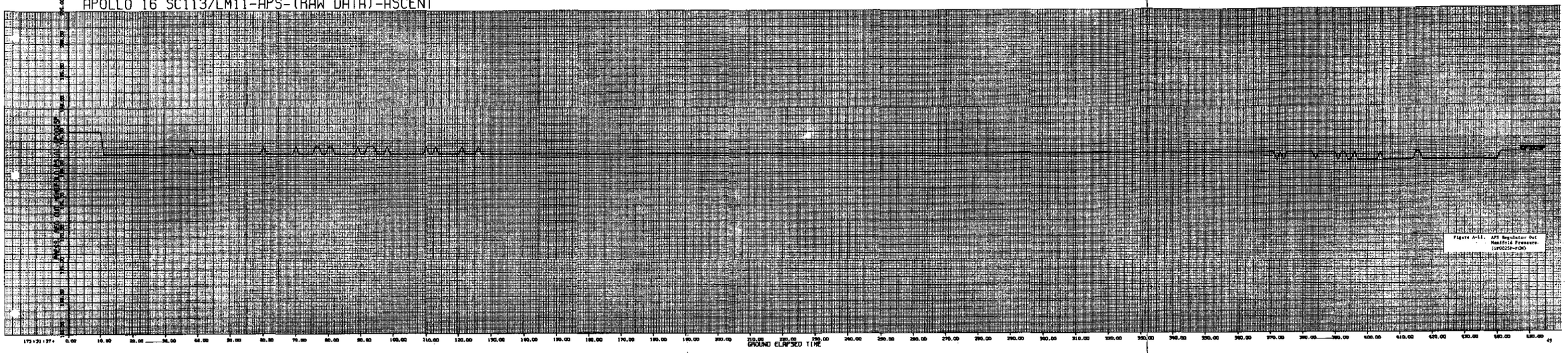


Figure A-11. APS Regulator Out Manifold Pressure. (GP5025P-FDM)



NASA-JSC

FOLDOUT FRAME

FOLDOUT FRAME